

Magnetic flux in the internetwork quiet Sun

E. V. Khomenko^{1,2}, M. J. Martínez González¹, M. Collados¹, A. Vögler³, S. K. Solanki³,
B. Ruiz Cobo¹, and C. Beck⁴

¹ Instituto de Astrofísica de Canarias, 38205 C/ vía Láctea, s/n, Tenerife, Spain

² Main Astronomical Observatory, NAS, 03680 Kyiv, Zabolotnogo Str. 27, Ukraine
e-mail: khomenko@iac.es

³ Max-Planck-Institut für Sonnensystemforschung, 37191 Katlenburg-Lindau, Germany

⁴ Kiepenheuer-Institut für Sonnenphysik, 79104 Freiburg, Germany

Received 1 March 2005 / Accepted 26 April 2005

Abstract. We report a direct comparison of the amplitudes of Stokes spectra of the Fe I 630 nm and 1.56 μm lines produced by realistic MHD simulations with simultaneous observations in the same spectral regions. The Stokes spectra were synthesized in snapshots with a mixed polarity magnetic field having a spatially averaged strength, $\langle B \rangle$, between 10 and 30 G. The distribution of Stokes V amplitudes depends sensitively on $\langle B \rangle$. A quiet inter-network region was observed at the German VTT simultaneously with TIP (1.56 μm) and POLIS (630 nm). We find that the Stokes V amplitudes of both infrared and visible observations are best reproduced by the simulation snapshot with $\langle B \rangle = 20$ G. In observations with 1'' resolution, up to 2/3 of the magnetic flux can remain undetected.

Key words. Sun: MHD – Sun: magnetic fields – Sun: infrared – Sun: polarization

1. Introduction

Magnetic fields in inter-network regions of the quiet solar atmosphere are difficult to accurately measure. As a consequence, measurements of the magnetic flux based on observations with different sensitivity and spatial resolution sometimes contradict each other. Thus, Domínguez Cerdeña et al. (2003) report a strong increase of the flux up to 17–21 G with increasing resolution from 1'' to 0''.5. At the same time, Lites & Socas-Navarro (2004) do not find such an increase and measured fluxes of about 8 G at 0''.6 resolution.

The measurements by Zeeman effect using different spectral lines also lead to different flux estimates. In the simultaneous observations in the visible and infrared Fe I lines reported by Sánchez Almeida et al. (2003b), the flux in both spectral ranges is not the same and amounts to 11 G (630.2 nm) and 6 G (1.5648 μm); even the polarity of the field in the same spatial point observed in the visible and infrared can be different. The flux obtained in the visible is larger than in similar ASP data (Lites & Socas-Navarro 2004) even though the resolution of the former observations was significantly lower (about 1''.4).

Applying the Hanle effect, which is not affected by polarity cancellations, Trujillo Bueno et al. (2004) report a substantially larger average magnetic field strength of 60 G (corresponding to a longitudinal flux of about 35 G). The Hanle effect is sensitive to weak turbulent fields, while the Zeeman effect is

not. This may cause an apparent contradiction between the two techniques.

Here, we perform a direct comparison of the amplitudes of simultaneously observed Stokes spectra of the Fe I 630 nm and 1.56 μm lines with those produced by realistic MHD simulations. By using simulation snapshots with different amounts of unsigned magnetic flux we are able to determine the level of flux best approximating both infrared and visible observations. The simulations allow us to estimate the “true” magnetic flux contained in the observed inter-network region even if the limited spatial resolution of the Zeeman-based observations allows only a small part of the total flux to be directly detected.

2. Observations

On August 17, 2003, a very quiet inter-network region at disc center was observed simultaneously in the infrared and visible spectral ranges using the polarimeters TIP (Martínez Pillet et al. 1999) and POLIS (Schmidt et al. 2000) attached to the Vacuum Tower Telescope at the Observatorio del Teide. The Stokes spectra of the 1.5648, 1.5652 μm and 630.1, 630.2 nm Fe I lines were recorded by scanning a 33'' \times 42'' region. The image was stabilized using a Correlation Tracker (Ballesteros et al. 1996), which also allowed accurate stepping perpendicular to the slit by 0''.4. The integration time at each slit position was around 27 s, which made it possible to achieve a noise level of 1.9×10^{-4} for TIP and 2.5×10^{-4} for POLIS (in terms of the

continuum intensity) and a spatial resolution of $1''.2$ and $1''.3$ respectively. The continuum contrast of granulation was 1.3% (infrared) and 2.7% (visible).

Dark current, flat-field, cross-talk corrections and demodulation were performed as usual. Continuum images were correlated to evaluate the differential displacement between the visible and infrared data due to atmospheric refraction effects. After the standard data reduction, a Principle Component Analysis (PCA) technique was used to eliminate noise (Rees et al. 2000). The filtered spectra have an extremely low noise level that was never achieved before in spectropolarimetric measurements with this spatial resolution ($5 \times 10^{-5} I_c$ for TIP and $6.5 \times 10^{-5} I_c$ for POLIS). In 80–90% of the field of view we measured amplitudes of Stokes V above a $3\text{-}\sigma$ threshold of 2×10^{-4} . This threshold level corresponds to $\langle B \rangle$ as low as 0.3 G. For details on observations and calibration see Martínez González et al. (2005) and Beck et al. (2005, in preparation).

3. MHD simulations and synthetic spectra

We have used the MURAM code, a 3D MHD code which includes non-grey radiative transfer, full compressibility, and the effects of partial ionization for the 11 most abundant chemical elements (Vögler et al. 2005). The size of the computational domain for the simulations considered here is $6000 \times 6000 \times 1400 \text{ km}^3$ with $288 \times 288 \times 100$ grid points. We consider here a simulation run that has a bi-polar structure of the magnetic field. The initial strength of the magnetic field introduced in the box was 200 G. Further details about the simulations can be found elsewhere (Vögler et al. 2005; Khomenko et al. 2005). The redistribution of the existing magnetic field by convective motions leads to the cancellation of elements with different polarities. This produces an almost exponential decrease with time of the average unsigned magnetic flux in the computational box. The snapshots used in the present work were taken when the average unsigned magnetic field strength in the box reached 30, 20 and 10 G at $\log \tau_{500} = -1$. In addition to that, a snapshot of a unipolar simulation with $\langle B \rangle = 10$ G is also considered (Shelyag et al. 2004).

The Stokes spectra of the Fe I 630.25 nm and $1.5648 \mu\text{m}$ lines formed at solar disc centre ($\mu = 1$) were calculated for every vertical column of the selected snapshots, under the assumption of local thermodynamic equilibrium. The synthetic spectra have a spatial grid resolution of 20 km and a continuum contrast of 9% (IR) and 16% (visible). In order to make these parameters comparable with the observations, we performed a convolution of the two-dimensional snapshots with a point-spread function. We used a combination of an Airy function appropriate for the VTT and a Lorentz function describing the image degradation by seeing (Shelyag et al. 2004). The contrast and the resolution of the smoothed images match the observations (Khomenko et al. 2005). After the smoothing, we added noise comparable to the observations and selected for the analysis only Stokes V profiles with amplitudes above 2×10^{-4} .

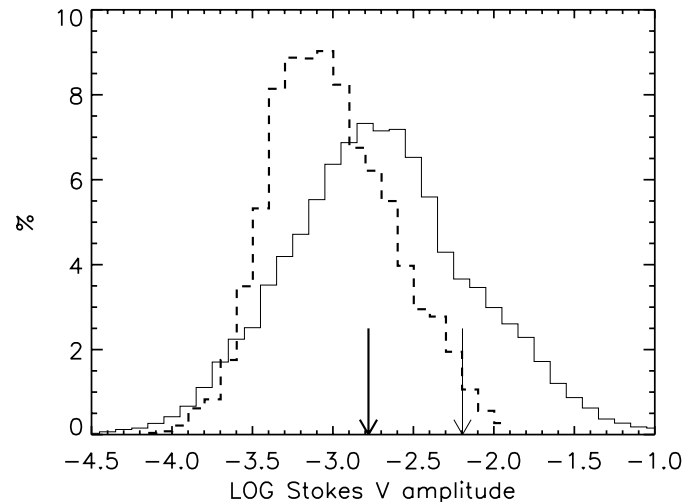


Fig. 1. Histograms of the amplitudes of Stokes V of Fe I 630.2 nm in the $\langle B \rangle = 20$ G simulation snapshot. Solid line: original resolution; dashed line: reduced resolution. Arrows indicate the mean values.

4. Original vs. reduced resolution

We verified that in the simulations, in most of the area, both Fe I lines are formed in the weak-field regime. Thus, the amplitudes of Stokes V are proportional to the longitudinal magnetic flux $\langle B_z \rangle$ contained in a resolution element and the original flux and those inferred from the synthetic magnetograms in these lines are nearly the same.

Figure 1 compares the distribution of Stokes V amplitudes of Fe I 630.2 nm with original and reduced resolution. The smearing causes a decrease of the average Stokes V amplitude in the box. This decrease is caused by several effects. Up to half of the average original amplitude can be lost by averaging profiles with significantly different displacements and splittings, such as those in granules and intergranules. Another source of loss is cancellation of elements with different polarities. While the first effect is always present in granulation, the second one depends on the spatial mixing of opposite polarities. In the case of the simulations, after reducing the resolution from 20 km to 700 km, the average polarization signal becomes about 3 times lower in both lines in all considered snapshots. It means that up to 2/3 of the original flux can remain undetected in $1''$ resolution observations if one uses Stokes V amplitudes as a measure of the magnetic flux. In observations with $0''.5$ resolution about 1/2 of the flux can be lost.

5. Simulations vs. observations

Figures 2 and 3 show maps of V amplitude of the simulations and observations, correspondingly. The stronger magnetic features are very similar in the visible and the infrared maps, in both Figs. 2 and 3. This demonstrates that both spectral lines “see” the same strong magnetic features. Strikingly, in both figures, there are many weak-flux concentrations that are present in the infrared and are absent in the visible. This is mainly a manifestation of the different Zeeman saturation regimes for the infrared and the visible lines.

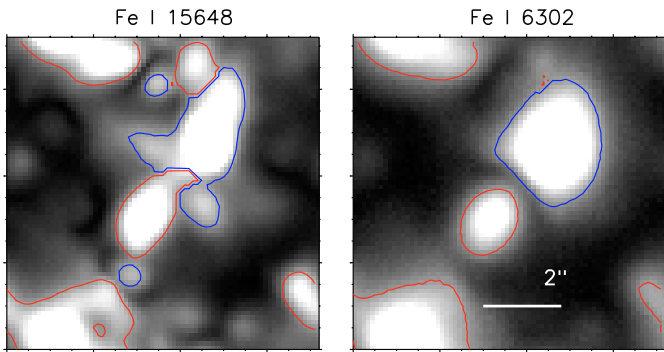


Fig. 2. Stokes V maps in the Fe I 1.5648 μm and 630.2 nm lines in a simulation snapshot with $\langle B \rangle = 20$ G. The grey scaling of both images is the same. The synthetic spectra are smoothed to the observed resolution. The color contours surround areas of a given polarity.

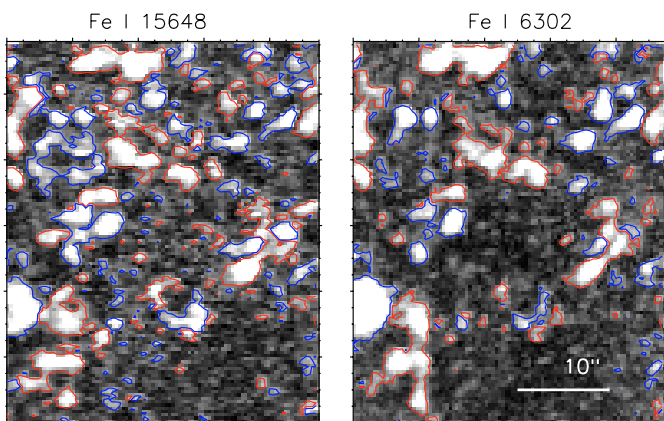


Fig. 3. Same as in Fig. 2 but now for the observations. Note the difference in spatial scale (*bottom of right panel*).

Sánchez Almeida et al. (2003b) found that 25% of the V profiles in the visible and infrared showed opposite polarities at the same spatial point. In our observations only 5.7% of the profiles follow this behaviour. In the simulations, such profiles make up 1–2% of all considered profiles. Whereas our observations were made under almost identical seeing conditions, they were different for the two wavelength bands for the observations of Sánchez Almeida et al. (2003b). We conclude that the appearance of the seemingly opposite polarities may be due to the difference in the spatial smearing (see also Khomenko et al. 2005).

Figure 4 shows a comparison between the observed and simulated Stokes V amplitudes. It reveals that the amplitudes resulting from the simulations are clearly too weak in the 10 G case (left panels) and too strong for the 30 G case (right panels). The best approximation to the observed histograms is achieved in the $\langle B \rangle = 20$ G case (central panels), suggesting that the “true” $\langle B \rangle$ contained in the observed inter-network region was close to 20 G.

This conclusion depends on the scales on which the polarities are mixed in the simulations. If the field in the Sun is mixed at smaller spatial scales than given by the simulations then more cancellations would occur and more flux would be

needed to make the amplitudes in the simulations equal to the observed ones (see for example the case of the turbulent dynamo simulations analyzed by Sánchez Almeida et al. 2003a, where only 10% of the original flux remains at 1 arcsec resolution). However, the fact that almost the entire shape of the histogram is matched and that the amplitudes of both lines can be reproduced simultaneously supports the conclusion that the field distribution in the simulations and observations should be similar. The ratio between the amplitudes in the IR and visible is an additional parameter constraining the magnetic field distribution and the flux level in the simulations. As follows from Fig. 5, it depends on the magnetic field in the model and is almost independent of the spatial resolution. In the observations, the average amplitudes of the infrared and the visible lines are close ($A_{6302}/A_{15648} \approx 1.2$), which is clearly not the case for the 10 G unipolar simulation. In the bi-polar simulation, the ratio of the amplitudes increases with $\langle B \rangle$ and is equal 0.9 (for 10 G), 1.1 (for 20 G) and 1.5 (for 30 G) (Fig. 4). Thus, the $\langle B \rangle = 20$ G case is, again, closest to the observations.

The case with a field strength of 20 G has an average longitudinal flux $\langle |B_z| \rangle$ of 11–15 G at $\log \tau_{500}$ from -1 to 0 . Taking into account the flux loss due to smearing, a $\langle |B_z| \rangle$ of about 4–5 G should be detected in 1'' resolution observations. In addition, because of the presence of noise, only the highest-amplitude signals are detectable in observations (covering some 60% of the area). The longitudinal flux averaged over these 60% of the highest-flux points in simulations at 1'' makes 6–9 G at $\log \tau_{500}$ from -1 to 0 and corresponds rather well to most observations (see Sánchez Almeida et al. 2003b; Khomenko et al. 2003; Lites & Socas-Navarro 2004). At 0'.5 resolution the latter value increases to 8–12 G. Thus, our results are in apparent contradiction with the high-resolution (0'.5) observations of Domínguez Cerdeña et al. (2003), who measured flux of 17 G from the 60% of the area covered by the signal above noise in Fe I 630.2 nm.

6. Conclusions

A comparison is performed between the amplitudes of the circular polarization signals in observations and realistic magneto-convection simulations. The observations used here are the first simultaneous observations in the visible and infrared Fe I spectral lines obtained with the same telescope. The extremely low noise in the observations allowed us to measure signals down to 2×10^{-4} in amplitude. These were found to cover 80–90% of the observed area. We find that under similar seeing conditions, Fe I 630 nm and Fe I 1.56 μm trace the same magnetic structures within the resolution element. The infrared line sees more weak-flux concentrations than the visible one. The amplitudes observed in the inter-network are incompatible with the amplitudes in a unipolar magnetic field simulation and are compatible with bi-polar simulations with an average magnetic field strength of $\langle B \rangle = 20$ G. Depending on the technique, up to 2/3 of this value can remain undetected in 1 arcsec resolution Zeeman observations. Further work (e.g. simulations with higher resolution) is required to identify the cause of the

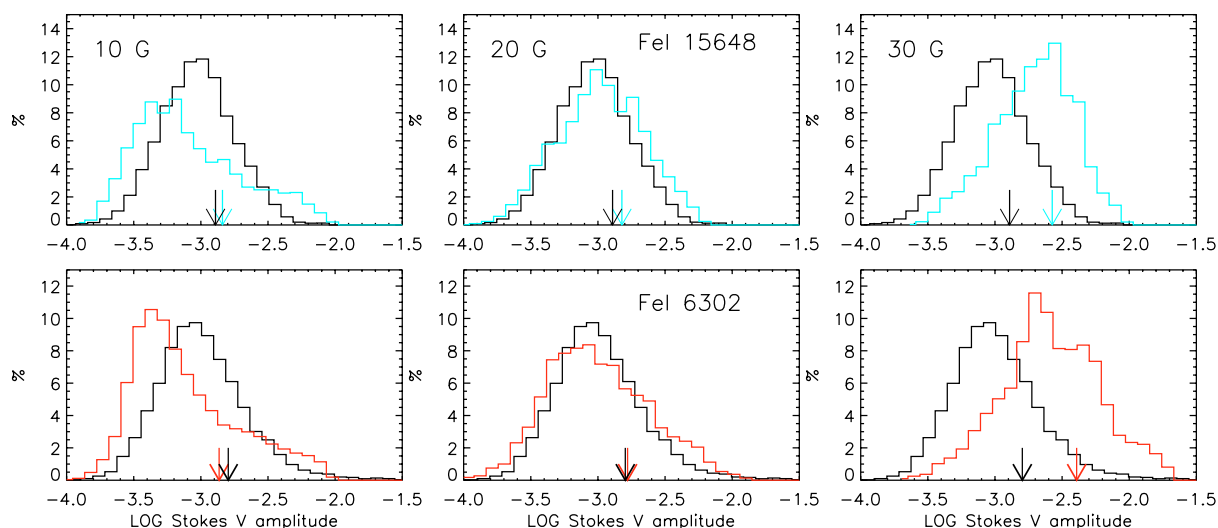


Fig. 4. Histograms of the amplitudes of Stokes V of Fe I $1.5648 \mu\text{m}$ (top) and Fe I 630.2 nm (bottom) lines. Blue and red line: simulations; black line: observations. From left to right simulation snapshots with $\langle B \rangle$ of 10 G, 20 and 30 G.

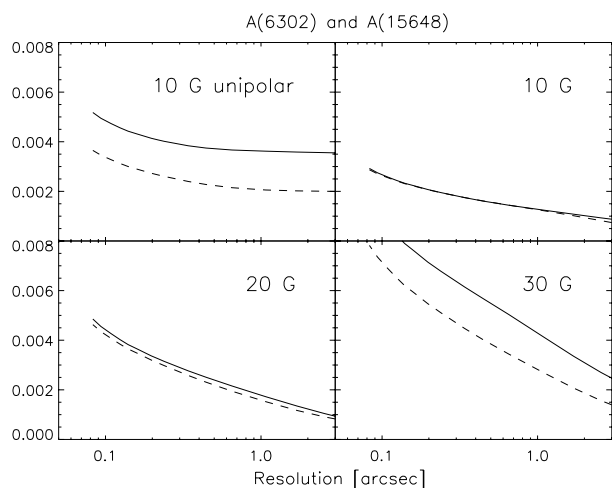


Fig. 5. Average Stokes V amplitudes of the Fe I $1.5648 \mu\text{m}$ (dashed) and 630.2 nm (solid) lines in simulations with different $\langle B \rangle$ as a function of the spatial resolution.

discrepancy between our results and the 3 times higher $\langle B \rangle$ value deduced by Trujillo Bueno et al. (2004).

Acknowledgements. This research was partially funded by INTAS grant 00-00084 and by the Spanish Ministerio de Educación y Ciencia through project AYA2004-05792.

References

- Ballesteros, E., Collados, M., Bonet, J. A., et al. 1996, *A&AS*, 115, 353
- Domínguez Cerdeña, I., Sánchez Almeida, J., & Kneer, F. 2003, *A&A*, 407, 741
- Khomenko, E. V., Collados, M., Solanki, S. K., Lagg, A., & Trujillo Bueno, J. 2003, *A&A*, 408, 1115
- Khomenko, E. V., Shelyag, S., Solanki, S. K., & Vögler, A. 2005, *A&A*, submitted
- Lites, B., & Socas-Navarro, H. 2004, *ApJ*, 613, 600
- Martínez Pillet, V., Collados, M., Sánchez Almeida, J., et al. 1999, in *High resolution solar physics: theory, observations and techniques*, ed. T. R. Rimmele, K. S. Balasubramaniam, & R. R. Radick, ASP Conf. Ser., 183, 264
- Rees, D. E., López Ariste, A., Thatcher, J., & Semel, M. 2000, *A&A*, 355, 759
- Sánchez Almeida, J., Domínguez Cerdeña, I., & Kneer, F. 2003b, *ApJ*, 597, L177
- Sánchez Almeida, J., Emonet, T., & Cattaneo, F. 2003a, *ApJ*, 585, 536
- Schmidt, W., Kentischer, T. J., & Lites, B. W. 2000, *POLIS: Instrument Description*, HAO-KIS
- Shelyag, S., Schüssler, M., Solanki, S. K., Berdyugina, S. V., & Vögler, A. 2004, *A&A*, 427, 335
- Trujillo Bueno, J., Shchukina, N. G., & Asensio Ramos, A. 2004, *Nature*, 430, 326
- Vögler, A., Shelyag, S., Schüssler, M., et al. 2005, *A&A*, 429, 335